Rms-flux relation of Cyg X-1 with *RXTE*: dipping and nondipping cases

Ya-Juan Lei, Li-Ming Song and Jin-Lu Qu
Laboratory for Particle Astrophysics, Institute of High Energy Physics, Chinese Academy of Sciences, 100049, Beijing, China; leiyj@mail.ihep.ac.cn

Cheng-Min Zhang
National Astronomical Observatories, Chinese Academy of Sciences, 100012, Beijing, China; zhangcm@bao.ac.cn

Mar 5, 2007

Abstract. The rms (root mean square) variability is the parameter for understanding the emission temporal properties of X-ray binaries (XRBs) and active galactic nuclei (AGN). The rms-flux relation with *Rossi X-ray Timing Explorer (RXTE)* data for the dips and nondip of black hole Cyg X-1 has been investigated in this paper. Our results show that there exist the linear rms-flux relations in the frequency range 0.1-10 Hz for the dipping light curve. Moreover, this linear relation still remains during the nondip regime, but with the steeper slope than that of the dipping case in the low energy band. For the high energy band, the slopes of the dipping and nondipping cases are hardly constant within errors. The explanations of the results have been made by means of the "Propagating Perturbation" model of Lyubarskii (1997).

1. Introduction

Aperiodic X-ray variability is a general characteristic of XRBs and AGN (e.g., van der Klis 1994; Vaughan et al. 2003a; McHardy et al. 2004; Uttley et al. 2005). The recent studies show that the linear rms-flux relation occurs in the X-ray light curves of XRBs and AGN over a broad range of time-scales, then this linear rms-flux relation is offset on the flux axis, which suggests the light curves to include at least two components: one component with a linear rms-flux relation and another with a constant rms to flux (Uttley & McHardy 2001; Gleissner et al. 2004). The fact of the same rms-flux relationship found in the light curves of XRBs and AGN suggests that this behavior is intrinsic to the accreting systems, and in addition the similar variability properties occur, as well, in neutron star (NS) and black hole (BH) XRBs (Uttley & McHardy 2001; Belloni et al. 2002) with the different X-ray spectra (e.g., Done & Gierlinski 2003). Therefore, investigating the X-ray vari-

ability would provide a probe in tracing the clues of the X-ray emission mechanisms of compact accreting systems.

Various models have been proposed to explain the shape of power-spectral density function (PSD) of XRBs, for example, the additive shot-noise models or flare models where the light curve is produced by a sum of shots or flares that trigger the avalanches of the smaller flares (similar to the model of Stern & Svensson (1996)), which is caused by the magnetic reconnection in the corona (Poutanen & Fabian 1999). This variability model is often mentioned as a "coronal flare" model (hereafter CF model, e.g., Uttley 2004). The PSD is a powerful tool to analyze the variability, however it confronts some limitations in distinguishing the models for aperiodic variability. While, these models seek to explain the observed PSD shapes by the distribution of shot time-scales and shot profiles which can fit any noise process PSD in theory (see, e.g., Miyamoto et al. 1988; Belloni & Hasinger 1990; Lochner et al. 1991; Negoro et al. 1995).

As indicated by Uttley & McHardy (2001), the linear rms-flux relation found in BH binary Cyg X-1 and NS binary SAX J1808.4-3658 could provide the strong constraints on models of variability, for example, the simple additive shot-noise or flare models cannot provide the linear rms-flux relation on short time-scale. Uttley (2004) demonstrates that the aperiodic variability showing the linear rms-flux relation in SAX J1808.4-3658 is coupled to the 401 Hz pulsation, implies this variability originates from the NS surface and not from the corona, which is most likely associated with the accretion flow. The "Propagating Perturbation" model (PP model for short) of Lyubarskii (1997) is a promised one, which ascribes the variability to the variations in accretion rate occurring at different radii (slow variations occurring at larger radii) while the perturbation propagates inwards and modulates the energy release in the X-ray-emitting region and results in the X-ray light curve. Besides successfully explaining the rms-flux relation, the PP model can also explain the spectral-timing properties of the variability (Kotov et al. 2001; Vaughan et al. 2003a; McHardy et al. 2004). Similar to the PP model, the exponential model of Uttley et al. (2005) can infer the linear rms-flux relation and a lognormal flux distribution, which is consistently associated with the observations.

X-ray dips often occur in the X-ray light curves of XRBs, and are suggested to be due to the absorption by matter passing through the line of sight to the X-ray emitting region (White et al. 1995). Thus, the research on the dips will provide us some information in the X-ray emitting region (e.g., Shirey et al. 1999; Asai et al. 2000; Church 2001).

In this paper, using $RXTE$ data of Cyg X-1, we study statistically the rms-flux relation over the frequency range 0.1-10 Hz of the dips

Table I. **The observations containing long term dips and data modes**

OBSID	Time	Data model
P10241	96-10-23 18:30:24 to 96-10-25 02:30:24	SB_250us_0_13_2s
P30158	97-12-14 08:48:14 to 97-12-30 05:30:14	SB_500us_0_13_2s
30161-01-01-000	97-12-28 13:56:00 to 97-12-28 21:03:07	SB_250us_0_13_2s
30161-01-01-00	97-12-28 21:03:07 to 97-12-29 00:18:14	SB_250us_0_13_2s
30161-01-02-000	98-11-13 13:10:33 to 98-11-13 21:10:33	SB_250us_0_13_2s
30161-01-02-00	98-11-13 21:10:33 to 98-11-13 22:00:14	SB_250us_0_13_2s
30161-01-02-01	98-11-13 22:40:32 to 98-11-13 23:34:14	SB_250us_0_13_2s

and nondip, respectively. In Sect. 2, we introduce the observational data and the method of calculating rms. The obtained results on the rms-flux relation are described in Sect. 3. The discussions about the rms-flux relation, including its slope and intercept, and models of X-ray variability are given in Sect. 4.

2. Observation and Data Reduction

We acquire the public archival data from *RXTE* Proportional Counter Array (PCA) observations of Cyg X-1, and choose the observations from April 15 of 1996 to March 22 of 1999 (PCA Epoch 3), which have the same channel-energy relationship. The observations of PCA Epoch 3 with the data modes SB_125us_0_13_2s, SB_250us_0_13_2s or SB_500us_0_13_2s are used. We extract the light curves of every OBSID with the standard 2 mode over the energy bands of 2-5 keV and 13-24 keV, where the hardness ratio is defined as the count rate ratios between 13-24 keV and 2-5 keV. We find the obvious long term dips (the duration of all the dips > 1000 s) in the observations P10241, P30158 and P30161, while in the low state (see Table 1). The P30161 contains many dips, so, which can be divided into two parts for analyzing. Figures 1-4 show the light curves and hardness ratio of the observations containing long term dip, and in the bottom panels of these four figures (hardness ratio) the dips are indicated by the arrows.

To determine whether the rms variability of a small segment of light curve depends on the mean flux of that segment for the dips and nondip, we cut the observed light curve with a resolution of 4 ms into the
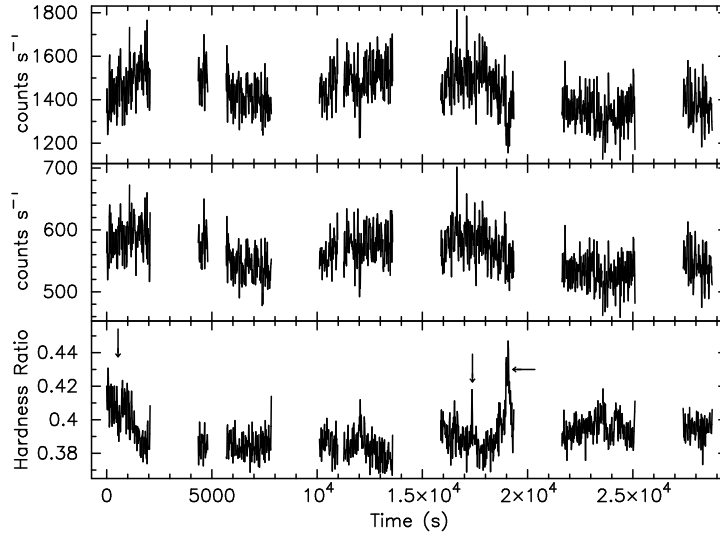
Figure 1. From top to bottom, the light curves of the 2-5 keV, 13-24 keV, and the hardness ratio, respectively, for OBSID P10241. The hardness ratio is defined as I(13-24 keV)/I(2-5 keV). Each point represents 16 s data from all five PCU detectors. The dips are indicated by the arrows.

segments of 32 s duration for which the source count rate is determined for computing the rms over the frequency range 0.1-10 Hz, respectively for the energy bands 2-5 keV and 13-24 keV. These segments are then assigned to their respective flux bins, and every flux bin contains at least 10 segments.

We adopt the method of Gleissner et al. (2004) to calculate rms, and it is determined for the chosen Fourier frequency interval. We construct the PSD of the individual light curve segment, applying the standard rms-squared normalization to the PSD (Miyamoto et al. 1992). We then average all the PSDs obtained from the segments in the same flux bin, and bin the averaged PSD over the chosen frequency range to yield the average power density $\langle P \rangle$ in that frequency range. Then, the absolute rms variability of the source, σ, is given as follows,

$$\sigma = [(\langle P \rangle - C_{Poisson})\, \Delta f]^{1/2}\, F \, , \tag{1}$$

where F is the mean count rate of every flux bin. C_{Poisson} is the Poisson noise level due to photon counting statistics, and Δf is the width of the chosen frequency range. The statistical uncertainty of the average PSD value, $\Delta \langle p \rangle$, is determined from the periodogram statistics (van der Klis 1989)
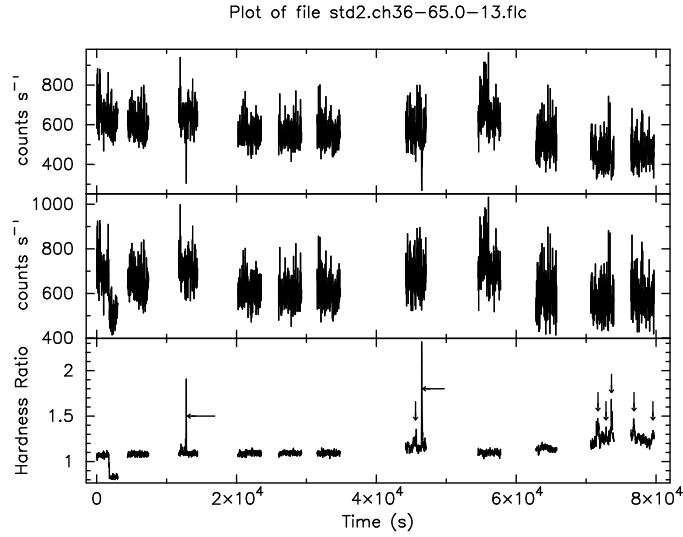
Plot of file std2.ch36−65.0−13.flc
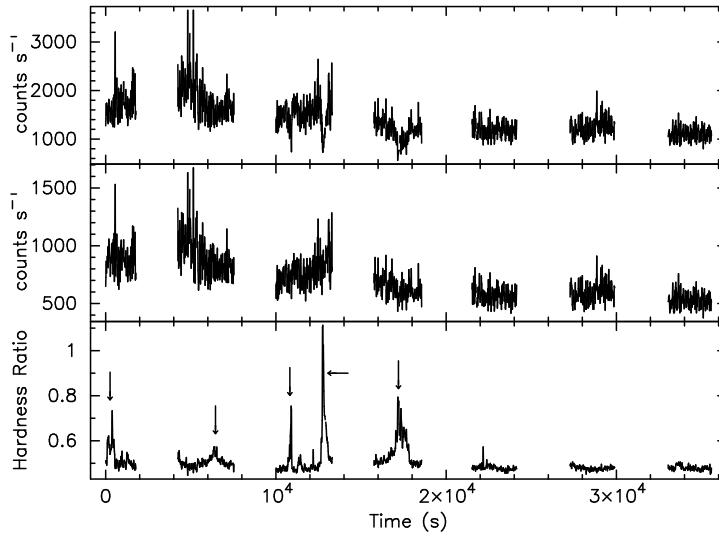

Figure 2. Similar to Fig. 1, but for OBSID P30158.

Figure 3. Similar to Fig. 1, but for OBSID 30161-01-01-000 and 30161-01-01-00.

$$\Delta \langle P \rangle = \frac{\langle P \rangle}{\sqrt{MW}} \ , \qquad (2)$$

where M is the number of segments used in determining the average rms value and W is the number of Fourier frequencies. The uncertainty of σ, $\Delta(\sigma)$, is then computed using the standard error propagation formula.
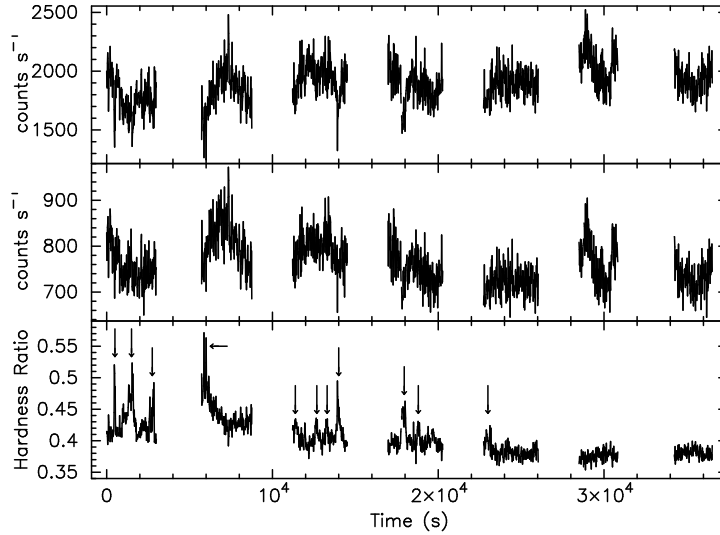
Figure 4. Similar to Fig. 1, but for OBSID 30161-01-02-000, 30161-01-02-00, 30161-01-02-01.

3. Results

For the dips and nondip of the studied observations, we analyze the data of the energy bands 2-5 keV and 13-24 keV, corresponding to the data modes. Their rms and flux values are plotted in Fig. 5-12. We use a function $\sigma = k(F - C)$ to fit the relations, where F is the mean flux of each flux bin and k (C)is the slope (intercept). The linear model provides a good fit to the data. As shown in Fig. 5-12, the fitted linear rms-flux relations do not pass through the coordinate origins, and there are the intercepts in the flux axis. Table 2 shows the values of k and C of all the studied observations.

For the energy band 2-5 keV, the photons are more absorbed by the obscuring matter. The slopes k of the dips are smaller than that of nondip for all the studied observations in the energy band, which implies that the obscuring matter affects the rms variability. The intercept C of the dips are also smaller than that of nondip (Table 2), indicating that the constant component is absorbed by the obscuring matter.

For the energy band 13-24 keV, except for the observation 30161-01-01-000 and 30161-01-01-00, the slopes k and intercepts C are constant within errors (Table 2), which can be due to that the high energy photons is hardly absorbed by the obscuring matter. For the observation 30161-01-01-000 and 30161-01-01-00, the obscuring matter could be so compact that affect the high energy photons, and lead to the decrease of
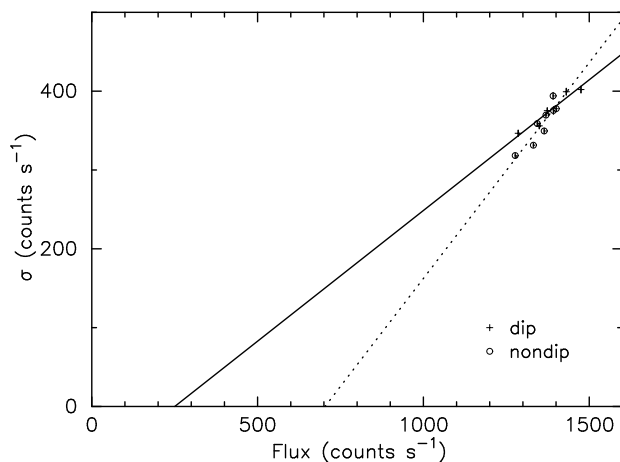
Figure 5. Root mean square amplitude σ of 0.1-10 Hz over the energy band 2-5 keV vs. X-ray flux for the dips and nondip of OBSID P10241, where the fitted linear relation $\sigma = k(F - C)$ is plotted with $k = 0.33 \pm 0.04$ and $C = 250 \pm 187$ for the dips and with $k = 0.55 \pm 0.05$ and $C = 703 \pm 130$ for the nondip, respectively. The cross (empty circle) stands for the dip (nondip).
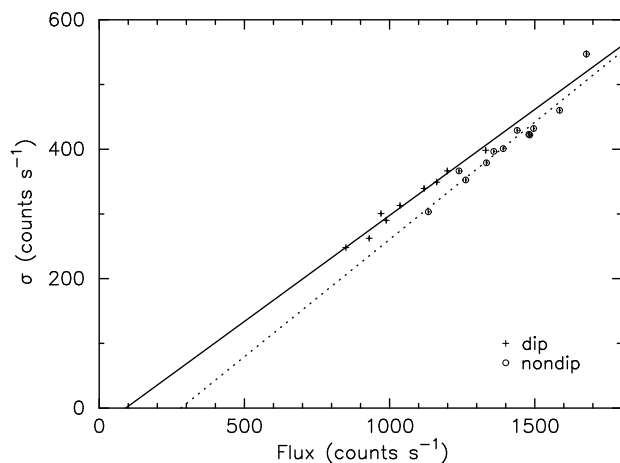

Figure 6. Similar to Fig. 5, but for OBSID P30158, $k = 0.33 \pm 0.01$ and $C = 92 \pm 34$ for the dips, and $k = 0.36 \pm 0.01$ and $C = 281 \pm 39$ for the nondip, respectively.

the slope k. In addition, for the nondip, our results show that the slopes k of 13-24 keV are smaller than those of 2-5 keV, which is consistent with the results of Gleissner et al. (2004) who deduce that the slope of the rms-flux relation decreases with the increase of the energy in the typical hard state observation of Cyg X-1.
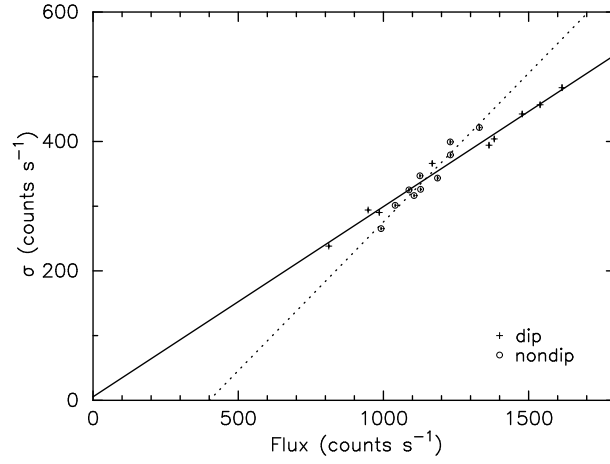
Figure 7. Similar to Fig.5, but for OBSID 30161-01-01-000 and 30161-01-01-00, $k = 0.29 \pm 0.01$ and $C = -20 \pm 24$ for the dips, and $k = 0.46 \pm 0.01$ and $C = 400 \pm 37$ for the nondip, respectively.
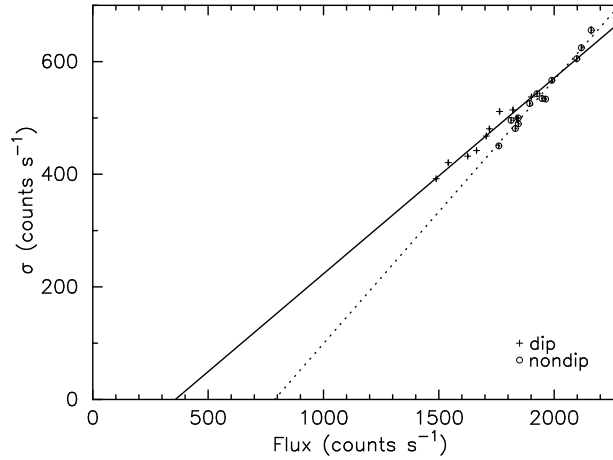

Figure 8. Similar to Fig. 5, but for OBSID 30161-01-02-000, 30161-01-02-00 and 30161-01-02-01, $k = 0.35 \pm 0.02$ and $C = 360 \pm 77$ for the dips, and $k = 0.47 \pm 0.02$ and $C = 788 \pm 83$ for the nondip, respectively.

Our results show that the obscuring matter does not significantly influence on the linear rms-flux relation, but reduces the rms variability of the low energy band. In general, the dips are suggested to be due to that the emission regions are obscured by the obscuring matter. Therefore, the obscuring matter could lead to the decrease of the rms variability.

Table II. **The slopes and intercepts of the linear rms-flux relations**

| OBSID	dip/nondip	slope (k)	intercept (C)	slope (k)	intercept (C)
		2-5 keV		13-24 keV	
P10241	dip	0.33 ± 0.04	250 ± 187	0.24 ± 0.05	12 ± 144
	nondip	0.55 ± 0.05	703 ± 130	0.33 ± 0.05	176 ± 98
P30158	dip	0.33 ± 0.01	92 ± 34	0.31 ± 0.02	13 ± 100
	nondip	0.36 ± 0.01	281 ± 39	0.32 ± 0.01	80 ± 19
30161-01-01-000	dip	0.29 ± 0.01	-20 ± 24	0.26 ± 0.01	-133 ± 35
30161-01-01-00	nondip	0.46 ± 0.01	400 ± 37	0.44 ± 0.02	189 ± 23
30161-01-02-000	dip	0.35 ± 0.02	360 ± 77	0.30 ± 0.03	240 ± 82
30161-01-02-00					
30161-01-02-01	nondip	0.47 ± 0.02	788 ± 83	0.33 ± 0.02	271 ± 51
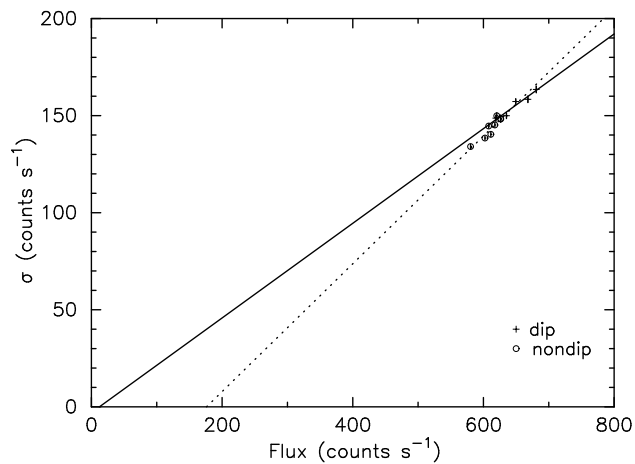
Figure 9. Root mean square amplitude σ of 0.1-10 Hz over the energy 13-24 keV vs. X-ray flux for the dips and nondip of OBSID P10241, where the fitted linear relation $\sigma = k(F - C)$ is plotted with $k = 0.24 \pm 0.05$ and $C = 12 \pm 144$ for the dips and with $k = 0.33 \pm 0.05$ and $C = 176 \pm 98$ for the nondip, respectively. The cross (empty circle) stands for the dip (nondip).
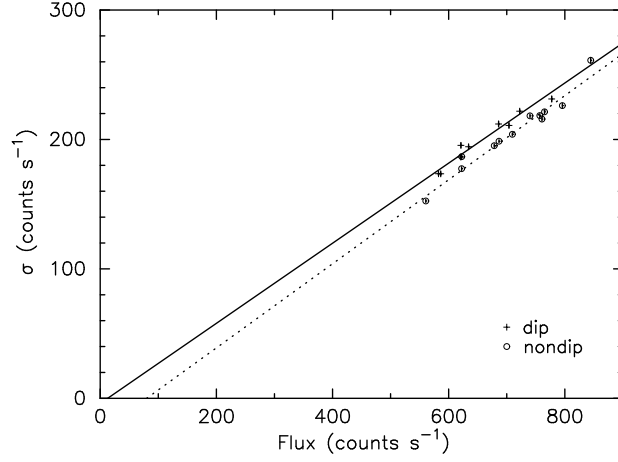
Figure 10. Similar to Fig. 9, but for OBSID P30158, $k = 0.31\pm0.02$ and $C = 13\pm100$ for the dips, and $k = 0.32 \pm 0.01$ and $C = 80 \pm 19$ for the nondip, respectively.
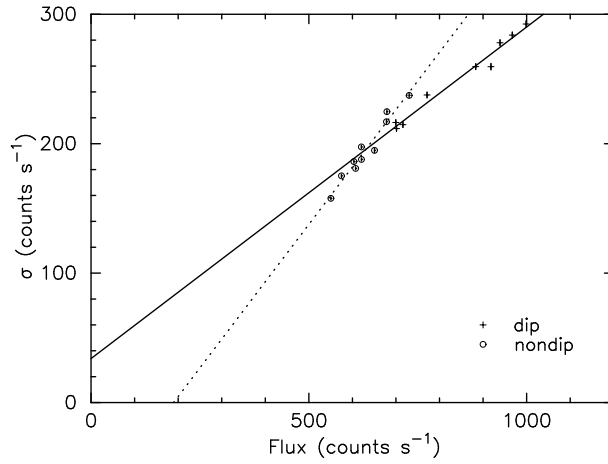

Figure 11. Similar to Fig.9, but for OBSID 30161-01-01-000 and 30161-01-01-00, $k = 0.26\pm0.01$ and $C = -20\pm24$ for the dips, and $k = 0.44\pm0.02$ and $C = 400\pm37$ for the nondip, respectively.

4. Discussion

4.1. Comparison with the results of *ASCA* observation

Bałucińska-Church et al. (1997) study the rms-flux relations in the energy bands 0.7-4 keV and 4-10 keV of Cyg X-1 with *ASCA*, and find that there are (no) dips over the 0.7-4 keV (4-10 keV) energy band (see Fig.1 of Bałucińska-Church et al. (1997)). Our results show that,
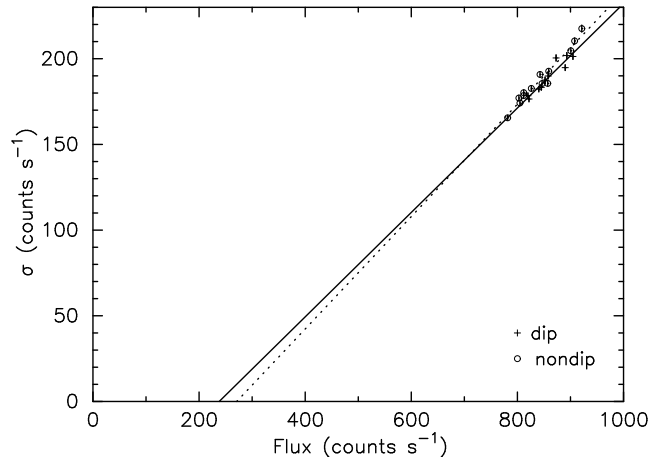
Figure 12. Similar to Fig. 9, but for OBSID 30161-01-02-000, 30161-01-02-00 and 30161-01-02-01, $k = 0.30 \pm 0.03$ and $C = 240 \pm 82$ for the dips, and $k = 0.33 \pm 0.02$ and $C = 271 \pm 51$ for the nondip, respectively.

for some observations, the dips exist in both 2-5 keV and 13-24 keV bands and the photons of the high energy band are also absorbed by the obscuring matter (Fig.1-4), which are not consistent with the results of Bałucińska-Church et al. (1997)who suggest that the X-ray emission region is not abscured in the high energy band.

The results from *ASCA* show that the rms variability is linearly related with the flux in the 0.7-4 keV band, then the rms variability is constant with the flux in the 4-10 keV band. Our results from *RXTE* show that the rms variability is linearly related with the flux in both 2-5 keV and 13-24 keV bands although both *ASCA* and *RXTE* observations are involved in the hard state of Cyg X-1.

The count rates of nondip data with *ASCA* are about 200 count s^{-1} in the 0.7-4 keV band, which are lower than the count rates from *RXTE* in the 2-5 keV band (also see, Fig. 1-4). Moreover, it is noticed that the count rates are as low as 60 count s^{-1} in the 4-10 keV band with *ASCA*, therefore the results by Bałucińska-Church et al. (1997) may be not conclusive.

4.2. THE RMS-FLUX RELATION AND MODELS OF X-RAY VARIABILITY

The linear rms-flux relations are observed in both XRBs and AGN, implying that the similar physical mechanisms work in these accreting systems. No doubt, the linear rms-flux relation provides the strong constraints on the models of the X-ray variability. Uttley & McHardy (2001) argue that a linear rms-flux relation in XRBs and AGN gets rid

of the additive shot-noise models, since these models treat the shots on all time-scales to be independent each other and cannot predict a linear rms-flux relation in a short time-scale. After analyzing the rms-flux relation of SAX J1808.4-3658, Uttley (2004) confirms that the variability could come from the accretion flow, not the accretion disk corona. In addition, the energy dependence characteristic of the variability disagrees with the conclusions of existing the extend corona (Maccarone et al. 2000; Focke et al. 2005). Furthermore, SOC (self-organized criticality in accretion flow) is also ruled out because it cannot produce the observed lognormal flux distribution (Uttley et al. 2005). Uttley et al. (2005) deduce that PP model seems to be a promising model at the present stage. In this model, the perturbations are treated to be produced at different radii in the accretion flow, and these perturbations can propagate inwards without being suppressed and then the perturbations at different radii can couple together. As pointed out, what could fulfill the possibility is a geometrically thick accretion flow where the accretion time-scales are relatively short so that the variations can propagate to the inner regions of the accretion flow without being significantly damped (Manmoto et al. 1996; Churazov et al. 2001; Arévalo & Uttley 2006). However, the origin of perturbation is not yet clear, although a variety of accretion instabilities could contribute to it (Frank et al. 1992). King et al. (2004) have shown that the magnetohydrodynamic turbulence can cause the accretion perturbations on the sufficiently long time-scales.

In the PP model, the X-ray variability of low (high) energy band is produced mostly in the outside (inside) of the accretion flow (Lyubarskii 1997). The phenomenological exponential model proposed by Uttley et al. (2005), which is mainly consistent with the conclusions of PP model, could reproduce the variability properties of the observed data. Our results show that the slope of the rms-flux relation decreases with the increase of the energy in the hard state of Cyg X-1 (also see, Gleissner et al. 2004). The PP model can provide an appropriate explanation: the photons of high energy band are produced in the inner accretion regime. The perturbations in the different outer radii of accretion flow propagate to the inner accretion flow and modulate the emission region, as a result, the amplitude of X-ray variability of high energy will increase. In fact, the perturbations from the different outer radii to the inner accretion flow could become stochastic in some extend. The increase of the stochastic component could weaken the variability of the inner X-ray emission region, which may result in the decrease of the rms variability in the high energy band.

Our results show that the values of k and C decrease from the nondip to dip in energy band 2-5 keV (see Table 2), suggesting the

optical thick obscuring matter locate outside of the emission region. In general, it is believed that the dips of Cyg X-1 are caused by the density enhancement in an inhomogeneous wind of the companion star or due to the partial obscuration of an extended X-ray emitting region by the optically thick "clumps" in the accretion flow (Feng & Cui 2002). Therefore, the reason for C decreasing could be due to the absorption of the obscuring matter to the constant component. On the other hand, the obscuring matter seems to add a little stochastic modulation to the intrinsic light curves, which could make the light curves a bit stochastic and then induce the decrease of k.

4.3. Changes of slope and intercept

The intercept C of the linear rms-flux relation sometimes is negative (also see,Gleissner et al. 2004). Therefore, C cannot simply represent a constant component to the light curve, but can represent a component with the constant rms. The slope k corresponds to an increase in the fractional rms of the linear rms-flux component of the light curve. For convenience, equivalently, the equation $\sigma = k(F - C)$ can be written as

$$\sigma = kF + \sigma_0 \, , \tag{3}$$

where $\sigma_0 = -kC$ is positive whenever $C < 0$, predicting $\sigma \to \sigma_0$ for $F \to 0$, which is unphysical. We adopt the assumption that $\sigma \to 0$ for $F \to 0$, which suggests that, when $\sigma < \sigma_0$, other variability process that does not obey the linear rms-flux relationship would be important and make $\sigma \to 0$ when $F \to 0$ (also see, Gleissner et al. 2004). When F is from $\simeq 0$ to a certain flux, suggesting that the value of k increase with the flux. When F is larger than a certain flux, the value of k is up to a constant, or the rms-flux becomes linear.

The PP model confirms that the X-ray variations produce at the different radii in the accretion flow, with the slower variations produced at larger radii. The accretion variations can then propagate to the small radii, then the variations at different radii, i.e., different time-scales, can couple together. In the emission region of high energy, the variations originate from the perturbations propagated from the different outer radii of accretion flow, and they couple with each other, which induces the increase of the stochastic component and the decrease of rms variability. However, the emission region of low energy is only modulated by the outermost variations, resulting in that the amplitude of variability is increasing with flux. Therefore, the slope of the high energy band is smaller that that of the low energy band.

Acknowledgments

References

Arévalo, P., & Uttley, P.:Investigating a fluctuating-accretion model for the spectral-timing properties of accreting black hole systems. Mon. Not. Roy. Astron. Soc 367, 801-804 (2006)

Asai, K., Dotani, T., Nagase, F., & Mitsuda, K.:Iron K Emission Lines in the Energy Spectra of Low-Mass X-Ray Binaries Observed with ASCA. ApJS 131, 571-591 (2000)

Balucinska-Church, M., Takahashi, T., Ueda, Y., Church, M. J., Dotani, T., Mitsuda, K., & Inoue, H.: The Cessation of Flickering during Dips in Cygnus X-1. Astrophys. J. 480, L115-L119 (1997)

Belloni, T., & Hasinger, G.:Variability in the noise properties of Cygnus X-1. Astron. Astrophys. 227, L33-L36 (1990)

Belloni, T., Psaltis, D., & van der Klis, M.:A Unified Description of the Timing Features of Accreting X-Ray Binaries. ApJ. 572, 392-406 (2002)

Churazov, E., Gilfanov, M., & Revnivtsev, M.: Soft state of Cygnus X-1: stable disc and unstable corona. Mon. Not. Roy. Astron. Soc 321, 759-766 (2001)

Church, M. J.: The emission regions in X-ray binaries: dipping as a diagnostic. Advances in Space Research. 28, 323-335 (2001)

Done, C., & Gierliński, M.: Observing the effects of the event horizon in black holes. Mon. Not. Roy. Astron. Soc 342, 1041-1055 (2003)

Feng, Y. X., & Cui, W.: Discovery of Two Types of X-Ray Dips in Cygnus X-1. Astrophys. J. 564, 953-961 (2002)

Focke, W. B., Wai, L. L., & Swank, J. H.: Time Domain Studies of X-Ray Shot Noise in Cygnus X-1. Astrophys. J. 633, 1085-1094 (2005)

Frank, J., King, A. R., Raine, D. J.: Accretion Power in Astrophysics, Cambridge (1992)

Gleissner, T., Wilms, J., Pottschmidt, K., Uttley, P., Nowak, M. A., & Staubert, R.: Long term variability of Cyg X-1. II. The rms-flux relation. Astron. Astrophys. 414, 1091-1104 (2004)

King, A. R., Pringle, J. E., West, R. G., & Livio, M.: Variability in black hole accretion discs. Mon. Not. Roy. Astron. Soc. 348, 111-122 (2004)

Kotov, O., Churazov, E., & Gilfanov, M.: On the X-ray time-lags in the black hole candidates. Mon. Not. Roy. Astron. Soc. 327, 799-807 (2001)

Lochner, J. C., Swank, J. H., & Szymkowiak, A. E.: Shot model parameters for Cygnus X-1 through phase portrait fitting. Astrophys. J. 376, 295-311 (1991)

Lyubarskii, Y. E.: Flicker noise in accretion discs. Mon. Not. Roy. Astron. Soc. 292, 679-685 (1997)

Poutanen, J., & Fabian, A. C.: Spectral evolution of magnetic flares and time lags in accreting black hole sources. Mon. Not. Roy. Astron. Soc. 306, L31-L37 (1999)

Maccarone, T. J., Coppi, P. S., & Poutanen, J.: Time Domain Analysis of Variability in Cygnus X-1: Constraints on the Emission Models. Astrophys. J. 537, L107-L110 (2000)

Manmoto, T., Takeuchi, M., Mineshige, S., Matsumoto, R., & Negoro, H.: X-Ray Fluctuations from Locally Unstable Advection-dominated Disks. Astrophys. J. 464, L135-L138 (1996)

McHardy, I. M., Papadakis, I. E., Uttley, P., Page, M. J., & Mason, K. O.: Combined long and short time-scale X-ray variability of NGC 4051 with RXTE and XMM-Newton. Mon. Not. Roy. Astron. Soc. 348, 783-801 (2004)

Miyamoto, S., Kitamoto, S., Iga, S., Negoro, H., & Terada, K.: Canonical time variations of X-rays from black hole candidates in the low-intensity state. Astrophys. J. 391, L21-L24 (1992)

Miyamoto, S., Kitamoto, S., Mitsuda, K., & Dotani, T.: Delayed hard X-rays from Cygnus X-1. Nature 336, 450-452 (1988)

Negoro, H., Kitamoto, S., Takeuchi, M., & Mineshige, S.: Statistics of X-Ray Fluctuations from Cygnus X-1: Reservoirs in the Disk?. Astrophys. J. 452, L49-L52 (1995)

Shirey, R. E., Levine, A. M., & Bradt, H. V.: Scattering and Iron Fluorescence Revealed during Absorption Dips in Circinus X-1. ApJ. 524, 1048-1058 (1999)

Stern, B. E., & Svensson, R.: Evidence for "Chain Reaction" in the Time Profiles of Gamma-Ray Bursts. Astrophys. J. 469, L109-L113 (1996)

Uttley, P.: SAX J1808.4-3658 and the origin of X-ray variability in X-ray binaries and active galactic nuclei. Mon. Not. Roy. Astron. Soc. 347, L61-L65 (2004)

Uttley, P., & McHardy, I. M.: The flux-dependent amplitude of broadband noise variability in X-ray binaries and active galaxies. Mon. Not. Roy. Astron. Soc. 323, L26-L30 (2001)

Uttley, P., McHardy, I. M., & Vaughan, S.: Non-linear X-ray variability in X-ray binaries and active galaxies. Mon. Not. Roy. Astron. Soc. 359, 345-362 (2005)

van der Klis, M.: Timing Neutron Stars, ed. H. Ögelman & E. P. J. van den Heuvel, NATO ASI No. C262 (Dordrecht: Kluwer Academic Publishers), 27 (1989)

van der Klis, M.: Similarities in neutron star and black hole accretion. ApJS 92, 511-519 (1994)

Vaughan, S., Fabian, A. C., & Nandra, K.: X-ray continuum variability of MCG-6-30-15. Mon. Not. Roy. Astron. Soc. 339, 1237-1255 (2003a)

White, N., Nagase, F., & Parmar, A. N.: X-ray Binaries, ed. W. G. H. Lewin, J. van Paradijs, & E. P. J. van den Heuvel (Cambridge: Cambridge Univ. Press),1 (1995)